On the impact of accurate radio link modeling on the performance of WirelessHART control networks

Yuriy Zacchia Lun[†], Claudia Rinaldi[‡], Amal Alrish[‡], Alessandro D'Innocenzo[‡], Fortunato Santucci[‡]

[†]*IMT School for Advanced Studies Lucca*, Italy - Email: yuriy.zacchialun@imtlucca.it
[‡]*Department of Information Engineering, Computer Science and Mathematics - University of L'Aquila*, Italy
Email: {claudia.rinaldi;alessandro.dinnocenzo;fortunato.santucci}@univaq.it, amal.alrish@graduate.univaq.it

***Abstract*—The challenges in analysis and co-design of wireless networked control systems are well highlighted by considering wireless industrial control protocols. In this perspective, this paper addresses the modeling and design challenge by focusing on WirelessHART, which is a networking protocol stack widely adopted for wireless industrial automation. Specifically, we first develop and validate a Markov channel model that abstracts the WirelessHART radio link subject to channel impairments and interference. The link quality metrics introduced in the theoretical framework are validated in order to enable the accurate representation of the average and extreme behavior of the radio link. By adopting these metrics, it is straightforward to handle a consistent finite-state abstraction. On the basis of such a model, we then derive a stationary Markov jump linear system model that captures the dynamics of a control loop closed over the radio link. Subsequently, we show that our modeling framework is able to discover and manage the challenging subtleties arising from bursty behavior. A relevant theoretical outcome consists in designing a controller that guarantees stability and improves control performance of the closed-loop system, where other approaches based on a simplified channel model fail.**

***Index Terms*—WirelessHART, Cyber-physical systems, MJLS.**

I. Introduction

Wireless networked control systems (WNCSs) are control systems where spatially distributed sensors, actuators, and controllers are connected through wireless networks. WNCS are becoming a fundamental infrastructure technology for critical control systems in automotive electrical systems, avionics, building management systems, and industrial automation [1], and their adoption is even speeding up with the spreading of most recent concepts of Internet of things (IoT) [2] and cyber-physical systems (CPSs) [3]. In order to cope with the automation-specific needs for quantifiably reliable, timely and efficient communication, the joint tuning of the critical interactive variables like sampling period, message delay, message dropout and network energy consumption is required [1], [4], [5], especially in the perspective of 5G URLLC (ultra-reliable low latency communication). Since every radio link of a typical industrial site is affected by harsh propagation (path loss and fading) and interference [6]–[9], this paper focuses on the modeling of a process that governs the message dropout, while taking into account complex interactions among several critical interactive system variables from [1], as represented in Fig. 1. In particular, we present a general framework for deriving an accurate radio link model (that is applicable to all data dropping links to and from a remote controller and/or state estimator), and then fix our attention on a link between the controller and actuator, to show that having a rigorous link model is essential for solving a wireless networked control problem. In order to convey the results to a broad audience, our presentation of the control problem is based on a state feedback, i.e. we make an idealistic assumption that all the system state variables are measured and sent to a controller over an error free link. This assumption can be readily relaxed by integrating the results from e.g. [10] at a cost of much more technical and tedious presentation.

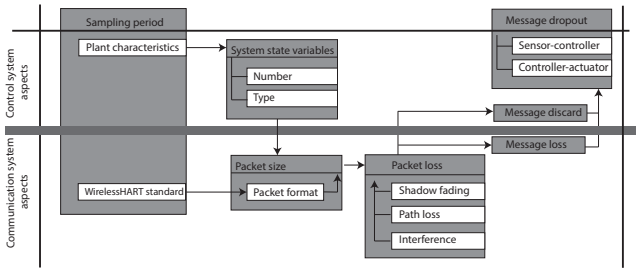

Fig. 1. Dependencies between critical system variables, [1].

While WNCSs are becoming increasingly popular in several application domains, they are still used only occasionally in current control loops in the process industry [7]: the lack of analytic methods for quantifying real-time performance in WNCSs has seriously hindered their adoption in industrial automation [11]. That is why nowadays the WNCSs design must explicitly deal with interdependencies between control and communication variables, motivating a cyber-physical co-design approach that integrates wireless networks models and control algorithms [11], [1]. More in detail, from the automatic control perspective, the wireless links are intended as the means to convey information among sensors, actuators, and computational units of WNCSs. Fading and interference

This research has received funding from the Sofidel SpA and Tuscany Region under POR FSE 2014-2020, Priority Axis A - Action A.2.1.7 - project SINCERA, number 172847, CUP D61J17000000004, and from the Italian Government under CIPE resolution n.135 (Dec. 21, 2012), project *INnovating City Planning through Information and Communication Technologies* (INCIPICT).

effects are typically abstracted in terms of frame/packet losses, that are modeled either as stochastic or deterministic phenomena [12]. The deterministic models proposed so far specify packet losses in terms of time averages or worst-case bounds on the number of consecutive dropouts (see e.g. [13]), while a vast amount of research considering stochastic models assumes memoryless packet drops, so that dropouts are realizations of a Bernoulli process (see e.g. [14]–[16]). The works that consider more general (bursty) packet losses use a transition probability matrix (TPM) of a stationary Markov chain (see e.g. the finite-state Markov modeling of multipath-induced fading channels in [17] and references therein) to describe the stochastic process that rules packet dropouts (see [10], [14], [18], [19]). In these works WNCSs with dropped (missing) packets are modeled as time-homogeneous Markov jump linear systems (MJLSs). It is noteworthy that most of the aforementioned works dealing with bursty packet losses (i.e., [10] and the references from [14]) tackle the problem of the stationary continuous state estimation, thus assuming the instantaneous availability of the jump variable. Such an assumption does not hold true for the networked control problem, where the operational modes are observed by controller via acknowledgements (ACKs). These ACKs are available only after the current decision on the gain to apply has been made and sent through the link, since the actual success of the transmission is not known in advance. The work [18] solves the problem of the optimal linear quadratic regulation of MJLSs with one time-step delayed mode observations, but it does not explore whether the provided solution effectively stabilizes a closed-loop system: this problem was recently solved in [19]. However, the models of packet losses assumed in automatic control literature are not consistently derived according to detailed channel models developed by the communications community and are typically oriented to oversimplify the actual behavior of the wireless link. Thus, we tackle the aforementioned issue by presenting a WNCSs modeling framework that accounts for both a detailed description of the wireless link and control plant characteristics. This provides useful insights onto the challenges of performance analysis and related design approach for WNCSs. As such challenges are well explained by considering wireless industrial control protocols, we focus on a networking protocol already developed for wireless industrial automation, i.e. WirelessHART [20], [21].

The main contribution of this paper is threefold. First, we provide in Section II a Markov model for a WirelessHART link subject to interference due to a neighboring network. Second, we define link quality metrics (LQMs) representing a powerful tool that is capable to easily evaluate and validate finite-state channel models to be used in the WNCSs applications. Lastly we show in Section IV that a MJLS model from Section III derived from a proper Markov channel model of a radio link permits to discover and overcome the challenging subtleties arising from a bursty behavior. Specifically, it can guarantee stability of the closed-loop WNCS where other approaches based on a simplified channel model fail. Our results are supported by a relevant numerical case study.

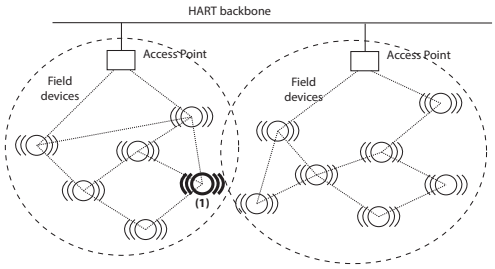

Fig. 2. Mutiple WirelessHART networks connected to the same backbone.

II. A MODEL FOR THE INTERFERED WIRELESSHART LINK

The process of derivation of an accurate radio link model consists of four major steps [22], that will be described in detail in the following subsections. Specifically, a thorough analysis of the communication scenario that identifies the relevant channel impairments and interferers, as will be introduced in Section II-A, is at the basis of our approach. Then an explicit form of the signal-to-interference-plus-noise ratio (SINR) can be derived by following the line of reasoning of Section II-B. This is the second step of our modeling process. The next step requires representing the SINR in a form of an approximating Gaussian process. Section II-C will show a systematic way of doing it. Once this implicit form of the SINR is available, it will be plain sailing to compute the related link quality metrics defined in Section II-D. Such metrics allow us to immediately assess the average and extreme behavior of the radio link. At this point, if not exactly the same, then a very similar behavior can be obtained from a finite-state Markov model of the communication link. Section II-E will provide all the necessary details on how to derive this model and its LQMs.

A. Scenario

The first step in developing our model is to study and analyze the communication scenario. In our reference scenario the link of interest within a WirelessHART network is interfered in a certain channel by a point to point communication belonging to another WirelessHART network. This scenario is shown in Fig. 2, where field device 1 is at the intersection of two zones.

In such a scenario the clear channel assessment (CCA) mode provides no benefit, since CCA mechanism is an optional coexistence feature targeting protocols and modulation standards different from WirelessHART. Therefore, it cannot address the case of users of different neighboring WirelessHART networks characterized by the same channel hopping sequence (which is the worst possible scenario that also accounts for malicious behaviors such as deliberate jamming).

Under the presented assumptions, the signal received by the reference user is

$$y(t) = y_0(t) + y_1(t) + n(t), \tag{1}$$

where $y_0(t)$ indicates the desired signal, $y_1(t)$ is the interference signal, while $n(t)$ is the additive white noise. In this paper, transmitted signals are assumed to be affected by path loss, shadow fading and residual power fluctuations left by power

control. The effect of multipath fading [23] is supposed to be compensated by the aforementioned power control.

The path loss, ς, is modeled as in the standard [24, p. 274] for 2.4 GHz:

$$\varsigma(d_i) = \begin{cases} 40.2 + 20\log_{10}(d_i) & \text{if } d \leq 8\ , \\ 58.3 + 33\log_{10}(\frac{d_i}{8}) & \text{otherwise,} \end{cases} \tag{2}$$

where d_i is the distance between the transmitter (Tx) i and the reference receiver (Rx).

The shadowing is expressed by its log-normal model [23], which has been investigated for indoor environments in [25], [26]. It is specified with the term $\beta_i(t)$, that has a Gaussian distribution with zero mean and variance $\sigma^2_{\beta_i}$ assumed constant during a symbol period. Here $i=0,1$ refers to the desired and interfering signals. It follows that the signal received by the reference user can be specified as

$$y(t)=\sum\nolimits_{i=0}^{1} \alpha_i e^{\frac{\beta_i(t)}{2}} s_i(t) + n(t), \tag{3}$$

where $\alpha_i = 10^{\frac{\varsigma(d_i)}{10}}$ is the path loss coefficient, $s_i(t)$ is the offset quadrature phase shift keying (OQPSK) direct sequence spread spectrum (DSSS) signal [27], that could be written as

$$s_i(t)=\sqrt{2P_i}a_i(t)[b_{I,i}(t)\cos(2\pi f_c t) - b_{Q,i}(t)\sin(2\pi f_c t)]\,,$$

with P_i being the transmitted (Tx) power over the i-th link, $a_i(t)$ the spreading signal, $b_{j,i}(t)$ the baseband data signal on the in-phase ($j=I$) or quadrature ($j=Q$) component, f_c the center frequency. Notably,

$$a_i(t)=\sum\nolimits_{l=-\infty}^{+\infty} \bar{a}_{i,l} p_{i,T_c}(t - lT_c), \tag{4}$$

$$b_{j,i}(t)=\sum\nolimits_{m=-\infty}^{+\infty} \bar{b}_{j,i,m} p_{i,T_s}(t - mT_s), \tag{5}$$

where $\{\bar{a}_{i,l}\}$ denotes the spreading sequences for the i-th link and $\{\bar{b}_{j,i,m}\}$ the binary data sequence for the i-th link on the I or Q component. Moreover, p_{i,T_c} and p_{i,T_s} are rectangular pulses with chip duration T_c and symbol duration T_s. We assume a coherent demodulation, allowing $y(t)$ to be decomposed into its I and Q components, $Y_I(t)$ and $Y_Q(t)$.

Then the next step of our modeling framework is to derive an explicit equation that represents the transmitted signal subject to the aforesaid channel imperfections and interference.

B. Explicit analytic model of SINR

Following [28], the output of the correlation receiver matched to the user signal is given by

$$Y_j(t)=\sum\nolimits_{i=0}^{1} Y_{j,i}(t) + N_j(t), \tag{6}$$

where $Y_{j,i}(t)$ and $N_j(t)$ are the components of $y_i(t)$ and $n(t)$,

$$Y_{j,i}(t)=\alpha_i e^{\frac{\chi_i(t)}{2}} \sqrt{\frac{P_i T_s}{2}} u_{j,i}, \tag{7}$$

with $u_{j,i}$ being the I or Q component of the transmitted complex symbol u_i, while $\chi_i(t)=\xi_i(t) + \beta_i(t)$, where $\xi_i(t)$ is the logarithmic residual power control error (PCE), envisaged in the WirelessHART standard [27], modeled by a zero-mean Gaussian process with variance $\sigma^2_{e_i}$ and autocovariance

$$c_{\xi_i}(\tau)=\sigma^2_{\xi_i} e^{-\frac{1}{2}\left(\frac{\tau}{\tau_{\xi_i}}\right)^2}, \tag{8}$$

where $\sigma_{\xi_i} = (\ln 10/10)\sigma_{e_i}$, while τ_{ξ_i} is the decorrelation time within which the PCE is significant [29].

The shadowing correlation is modeled as in [30]: if d_{c_i} denotes the typical decorrelation decay distance and v_i indicates the device speed, then

$$c_{\beta_i}(\tau)=\sigma^2_{\beta_i} e^{-\frac{1}{2}\left(\frac{v_i \tau}{d_{c_i}}\right)^2}. \tag{9}$$

Thus, the SINR (which will be denoted by Γ in logarithmic scale, and by γ when using the power value, $\Gamma \triangleq 10\log_{10}(\gamma)$ [dB]) conditioned to PCEs and shadowing, and assuming $\sqrt{u^2_{Q,i} + u^2_{I,i}} = 1$, is

$$\begin{aligned} \gamma(t) &= \frac{\sqrt{Y^2_{I,0}(t) + Y^2_{Q,0}(t)}}{\sqrt{\frac{N_0 T_s}{4} + \mathrm{var}\left\{\sqrt{Y^2_{I,1}(t) + Y^2_{Q,1}(t)}\right\}}} \\ &= \sqrt{\frac{P_0 e^{\chi_0(t)} \alpha_0^2}{\frac{N_0}{4} + \frac{8}{3G} P_1 e^{\chi_1(t)} \alpha_1^2}}, \end{aligned} \tag{10}$$

where the expectations are taken with respect to carrier phases, time delays, data symbols but not with respect to random processes vectors $\boldsymbol{\xi}(t) = (\xi_0(t), \xi_1(t))$, $\boldsymbol{\beta}(t) = (\beta_0(t), \beta_1(t))$. N_0 denotes the noise spectral density, $G = WT_s$ is the processing gain, W is the bandwidth, $1/T_s$ is the symbol rate.

The following step of our modeling process is finding a tractable representation of the explicit analytic model of SINR. To perform that, we can approximate it with another random process, (e.g. log-normal process) and then apply moment matching approach to get the signal statistics.

C. Implicit analytic model of SINR

Following [31], we let $\Gamma(t) = \mathrm{L}^{-1/2}(t)$, where due to the properties of the random prcesses involved, $\mathrm{L}^{-1/2}(t)$ is seen as a weighted sum of randomly correlated log-normal processes. This is valid also for $\mathrm{L}(t)$, which could be expressed as

$$\mathrm{L}(t) = \mathrm{D} e^{-\chi_0(t)} + \mathrm{B} e^{\chi_1(t) - \chi_0(t)}, \tag{11}$$

$$\mathrm{D} = \frac{N_0}{4\alpha_0^2 P_0}, \quad \mathrm{B} = \frac{8 P_1 \alpha_1^2}{3 G P_0 \alpha_0^2}. \tag{12}$$

So, we apply the moment matching technique [31] as follows. Let $Z(t)$ be a Gaussian process with mean η_Z, variance σ^2_Z, and autocovariance $c_Z(\tau)$, such that $\mathrm{L}(t) \approx e^{Z(t)}$. Let $\mathrm{E}\{\cdot\}$ denote the mathematical expectation. Then

$$\begin{cases} \mathrm{M}_1 = \mathrm{E}\{\mathrm{L}(t)\} \triangleq \mathrm{E}\{e^{Z(t)}\} = e^{\eta_Z + \frac{1}{2}\sigma^2_Z}, \\ \mathrm{M}_2(\tau) = \mathrm{E}\{\mathrm{L}(t)\mathrm{L}(t+\tau)\} \triangleq \mathrm{E}\{e^{Z(t) + Z(t+\tau)}\} \\ \qquad\quad = e^{2\eta_Z + \sigma^2_Z + c_Z(\tau)}, \\ \mathrm{M}_2(0) = e^{2\eta_Z + 2\sigma^2_Z}. \end{cases} \tag{13}$$

Solving the equations defining M_1, $\mathrm{M}_2(\tau)$ and $\mathrm{M}_2(0)$ in η_Z, σ^2_Z and $c_Z(\tau)$ yields the following expressions:

$$\begin{cases} \eta_Z = 2\ln \mathrm{M}_1 - \frac{1}{2}\ln \mathrm{M}_2(0), \\ \sigma^2_Z = \ln \mathrm{M}_2(0) - 2\ln \mathrm{M}_1, \\ c_Z(\tau) = \ln\left(\frac{\mathrm{M}_2(\tau)}{\mathrm{M}_1^2}\right). \end{cases} \tag{14}$$

Since $\xi_i(t)$ and $\beta_i(t)$ are zero mean independent processes,

$$\begin{cases} \mathrm{M}_1 = \mathrm{D} e^{\frac{1}{2}(\sigma^2_{\xi_0} + \sigma^2_{\beta_0})} + \mathrm{B} e^{\frac{1}{2}(\sigma^2_{\xi_1} + \sigma^2_{\beta_1} + \sigma^2_{\xi_0} + \sigma^2_{\beta_0})}, \\ \mathrm{M}_2(\tau) = e^{\sigma^2_{\chi_0} + c_{\chi_0}(\tau)}\Big[\mathrm{D}^2 + 2\mathrm{D}\mathrm{B} e^{\frac{1}{2}\sigma^2_{\chi_1}} + \mathrm{B}^2 e^{\sigma^2_{\chi_1} + c_{\chi_1}(\tau)}\Big], \end{cases}$$

where $c_{\chi_i}(\tau)=c_{\xi_i}(\tau)+c_{\beta_i}(\tau)$, $\sigma^2_{\chi_i}=\sigma^2_{\xi_i}+\sigma^2_{\beta_i}$, for $i=0,1$.

Given the relation between $Z(t)$ and $\mathrm{L}(t)$, few manipulations bring to

$$\Gamma(t)=\kappa Z(t) \quad \text{where} \quad \kappa=-\frac{5}{\ln 10}, \tag{15}$$

so that $\Gamma(t)$ is a Gaussian process with mean, variance and autocovariance

$$\begin{cases} \eta_\Gamma=\kappa\eta_Z, \\ \sigma^2_\Gamma=\kappa^2\sigma^2_Z, \\ c_\Gamma(\tau)=\kappa^2 c_Z(\tau). \end{cases} \tag{16}$$

In the rest of this paper, we will denote it by $\Gamma(t)\sim\mathcal{N}(\eta_\Gamma,\sigma^2_\Gamma)$, if the relevant values of $c_\Gamma(\tau)$ will be given.

The closed-form expression (16) evolves at the symbol rate and encompasses the stochastic characteristics of the WirelessHART link for the considered scenario. It allows us to define some important quality metrics describing the lossy communication link, which will be expounded in the next subsection. However, to define these quality metrics formally, we need to pay attention to the control-related data messages and not just to individual symbols.

In networks based on IEEE 802.15.4 compatible hardware the SINR estimation is performed for each received packet during link quality indicator (LQI) measurement [24, p. 65]. Since OQPSK modulation encodes two bits per symbol, the number of symbols within a control-related frame is $(\ell_F/2)$, where ℓ_F indicates the number of bits in the *frame*. Therefore, the estimated $\Gamma(t)$ refers to a block of $(\ell_F/2)$ symbols. WirelessHART-based WNCSs send data at a rate that is inversely proportional to the update period of the dedicated Publish data messages [21, p. 248]. Thus, between two control-related data transmissions the presented link has approximately ℓ_{E} *evolutions* which could be expressed as

$$\ell_{\mathrm{E}}=\mathrm{round}\left(\frac{2T_u}{\ell_{\mathrm{F}}T_s}\right). \tag{17}$$

For $\ell_{\mathrm{F}}=208$ bits, $T_u=0.1$ s, and $1/T_s=62.5$ kHz we have that $\ell_{\mathrm{E}}=\mathrm{round}\,(60.096)=60$. In general, we need to

$$\text{compute values of } c_\Gamma(\tau) \text{ for } \tau=k\ell_{\mathrm{E}}+1,\ k\in\mathbb{N},$$

in order to evaluate the time correlations at the time scale of the control application.

D. Link quality metrics of the analytic model

Since currently WirelessHART does not provide for implementation of the forward error correction, even one erroneous bit leads to a corrupted WirelessHART data packet. According to the IEEE 802.15.4-2006 standard [24], which provides the physical layer of WirelessHART, the *bit* error ratio (BER, $\mathrm{R_b}$) depends only on the power value γ of SINR [24, p. 268].

Therefore, the *packet* error rate (PER, $\mathrm{R_p}$) is related to SINR through BER, where $\gamma\in(0,\infty)$, and both $\mathrm{R_b}(\gamma)\in[0,0.5]$, $\mathrm{R_p}(\gamma)\in[0,1]$ are continuous monotonically non-increasing

$$\mathrm{R_p}(\gamma)=1-(1-\mathrm{R_b}(\gamma))^{\ell_{\mathrm{F}}},$$
$$\mathrm{R_b}(\gamma)=\frac{1}{30}\sum\nolimits_{i=2}^{16}(-1)^i\binom{16}{i}e^{\left(20\gamma\frac{1-i}{i}\right)}. \tag{18}$$

An unreliable communication link can be characterized by the likelihood of the information losses and by the maximum number of consecutive dropouts [12], which in stochastic framework have a non-negligible probability of occurrence. The PER defined on the presented implicit *analytic* model of SINR encompasses this information, since the probability density function $f_\Gamma(\cdot)$ of the SNIR is known, and $\mathrm{R_p}(\cdot)$ is a continuous function defined on the range of Γ: by the law of the unconscious statistician, the expected value of the PER, denoted by η_{A}, can be obtained as

$$\eta_{\mathrm{A}}=\int_{-\infty}^{+\infty}\mathrm{R_p}(10^{\frac{\zeta}{10}})f_\Gamma(\zeta)\,d\zeta, \tag{19}$$

while its variance, indicated by σ^2_{A}, can be computed as:

$$\sigma^2_{\mathrm{A}}=\int_{-\infty}^{+\infty}\mathrm{R_p^2}(10^{\frac{\zeta}{10}})f_\Gamma(\zeta)\,d\zeta-\eta^2_{\mathrm{A}}. \tag{20}$$

In practical applications the PER is considered negligible when it is smaller than a specified threshold ε_{p}, which may be as small as the machine epsilon. Since $\mathrm{R_p}(\cdot)$ is a continuous monotonically non-increasing function of $\Gamma(t)$, any value υ_Γ of the SINR such that $\upsilon_\Gamma\geq\upsilon^\star_\Gamma(\varepsilon_{\mathrm{p}})$, where

$$\upsilon^\star_\Gamma(\varepsilon_{\mathrm{p}})\triangleq\min_{\upsilon}\mathrm{R_p}(\upsilon)=\varepsilon_{\mathrm{p}} \tag{21}$$

almost surely has PER equal to zero. The value of $\upsilon^\star_\Gamma(\varepsilon_{\mathrm{p}})$ can be easily computed by one of the standard root-finding algorithms, and the probability of having a non-negligible PER is given by the value of the cumulative distribution function $F_\Gamma(\cdot)$ of the $\Gamma(t)$ in $\upsilon^\star_\Gamma(\varepsilon_{\mathrm{p}})$. When there is a time correlation, i.e., when $c_\Gamma(k\ell_{\mathrm{E}}+1)\neq 0$ for all $k\in\mathbb{N}$, the formal definition of the probability of having a packet error *burst* of length ℓ_{B} relies on the notion of the multivariate normal cumulative distribution function [32]

$$F_{\Gamma_1\cdots\Gamma_{\ell_{\mathrm{B}}}}(\upsilon\mathbf{1})\triangleq\frac{1}{\sqrt{|\boldsymbol{\Sigma}|(2\pi)^{\ell_{\mathrm{B}}}}}\int_{-\infty}^{\upsilon-\eta_\Gamma}\cdots\int_{-\infty}^{\upsilon-\eta_\Gamma}e^{-0.5\mathbf{z}'\boldsymbol{\Sigma}^{-1}\mathbf{z}}dz_1\cdots dz_{\ell_{\mathrm{B}}},$$

where $\mathbf{1}$ denotes the column vector of the appropriate length with all entries being equal to the scalar 1, $|\cdot|$ indicates the determinant, $'$ symbolizes the operation of transposition, while $\boldsymbol{\Sigma}$ is a symmetric, positive definite covariance matrix, whose entry in position (i,j) is the value of $c_\Gamma(\tau)$, for $\tau=(i-j)\ell_{\mathrm{E}}+1$, if $i\neq j$, and $\tau=0$ otherwise. We observe that $\boldsymbol{\Sigma}$ is banded [32], i.e., it satisfies the condition $c_\Gamma(\tau)=0$ whenever $\tau>l$ for some $l\geq 0$. This special correlation structure of $\boldsymbol{\Sigma}$ allows efficient computation [33] of $F_{\Gamma_1\cdots\Gamma_{\ell_{\mathrm{B}}}}\big(\upsilon^\star_\Gamma(\varepsilon_{\mathrm{p}})\mathbf{1}\big)$.

Since the probability of a packet error burst is negligible when it is smaller than a specified threshold ε_{B}, the largest number of consecutive dropouts with a non-negligible probability of occurrence $\ell^\star_{\mathrm{B}}(\varepsilon_{\mathrm{B}},\varepsilon_{\mathrm{p}})$ can be computed iteratively:

$$\begin{aligned}\ell^\star_{\mathrm{B}}(\varepsilon_{\mathrm{B}},\varepsilon_{\mathrm{p}})\triangleq\max_{\ell_{\mathrm{B}}}&F_{\Gamma_1\cdots\Gamma_{\ell_{\mathrm{B}}}}\big(\upsilon^\star_\Gamma(\varepsilon_{\mathrm{p}})\mathbf{1}\big)\ \text{ subject to}\\ &F_{\Gamma_1\cdots\Gamma_{\ell_{\mathrm{B}}}}\big(\upsilon^\star_\Gamma(\varepsilon_{\mathrm{p}})\mathbf{1}\big)\geq\varepsilon_{\mathrm{B}}.\end{aligned} \tag{22}$$

When $l\leq\ell_{\mathrm{E}}$, we have that $F_{\Gamma_1\cdots\Gamma_{\ell_{\mathrm{B}}}}\big(\upsilon^\star_\Gamma(\varepsilon_{\mathrm{p}})\mathbf{1}\big)=F_\Gamma\big(\upsilon^\star_\Gamma(\varepsilon_{\mathrm{p}})\big)^{\ell_{\mathrm{B}}}$, so it is easy to verify that

$$\ell^\star_{\mathrm{B}}(\varepsilon_{\mathrm{B}},\varepsilon_{\mathrm{p}})=\mathrm{ceil}\left(\frac{\ln(\varepsilon_{\mathrm{B}})}{\ln\left(\frac{1}{2}\left(1+\mathrm{erf}\left(\frac{\upsilon^\star_\Gamma(\varepsilon_{\mathrm{p}})-\eta_\Gamma}{\sigma_\Gamma\sqrt{2}}\right)\right)\right)}\right), \tag{23}$$

where $\mathrm{ceil}(\cdot)$ and $\mathrm{erf}(\cdot)$ are the ceiling and error functions, respectively. The presented closed form expression (23) of

$\ell^{\star}_{\rm B}(\varepsilon_{\rm B},\varepsilon_{\rm p})$ provides a useful lower bound on its true value (22).

In summary, the LQMs characterizing the analytic model of the WirelessHART link are listed in Table I. They will be compared with the LQMs of finite-state abstractions of the analytic model in order to validate these abstractions and provide guidelines on the choice of parameters defining the aforementioned abstractions.

TABLE I
ANALYTIC LQMS.

Link quality metric	Notation
The packet error probability (PEP)	$\eta_{\rm A}$
The PER's variance	$\sigma^2_{\rm A}$
The maximum number of consecutive dropouts	$\ell^{\star}_{\rm B}(\varepsilon_{\rm B},\varepsilon_{\rm p})$

E. Finite-state Markov model

The analytic model of a communication link presented in the previous subsections is defined on a continuous state-space, where the SINR is defined on the set of all ordinary real numbers, namely $\Gamma(t)\in(-\infty,+\infty)$. Nevertheless, there are several application scenarios (e.g. decoding in channels with memory, adaptive transmission, as well as modeling of lossy communication link's error bursts) where using a finite number of channel states can be more advantageous [17].

The coarsest abstraction of the analytic model collapses the infinite-dimensional state-space into one state with a representative PEP (given by $\eta_{\rm A}$), which may be seen as a probability of the packet loss event in the Bernoulli distribution. If random variables are *jointly normal* and uncorrelated, then they are independent: if the autocovariance of the Gaussian process representing the evolution of $\Gamma(t)$ has $c_\Gamma(\tau)\approx 0$ for all $\tau>\ell_{\rm E}$, then the i.i.d. Bernoulli model introduces no conservatism.

In a more accurate finite-state Markov channel abstraction the range of SINR is divided into several consecutive regions, to each of which is associated a certain representative PEP. A region i of the values of SINR is mapped into a state $\mathbf{s}_i$ of the related Markov chain and is delimited by two thresholds ζ_i and ζ_{i+1} belonging to the set of extended reals. The steady state probability $\mathbf{p}_i$ of a state $\mathbf{s}_i$ is the probability that the SINR is between thresholds of the region, which is given by

$$\mathbf{p}_i=\int_{\zeta_i}^{\zeta_{i+1}} f_\Gamma(\zeta)d\zeta, \tag{24}$$

while the PEP associated to the same state is given by the expected value of the PER within the respective region, i.e.

$$\eta^{(i)}_{\rm M}=\frac{1}{\mathbf{p}_i}\int_{\zeta_i}^{\zeta_{i+1}} {\rm R_p}(10^{\frac{\zeta}{10}})f_\Gamma(\zeta)\,d\zeta. \tag{25}$$

The TPM of the Markov channel may be obtained from the level crossing rate (LCR) analysis [17]. This analysis considers the number of times per second the SINR crosses each threshold (with the obvious exception of the two thresholds having the values equal to $\pm\infty$) in a downward direction, divided by the average number of symbols per second the SINR falls in the interval associated to state of interest (i.e. $(\mathbf{p}_i/T_s)=62500\mathbf{p}_i$ for the WirelessHART, [24, p. 49]). In particular, the well known expressions for the LCR analysis of a Gaussian process [34] may be used as follows. Let $\rm R_c$ denote the rate of *crossing* a certain threshold. Then

$${\rm R_c}(\zeta_i)=\frac{1}{2\pi}\sqrt{\frac{\ddot{c}_\Gamma(0)}{c_\Gamma(0)}}\,e^{-\frac{(\zeta_i-\eta_\Gamma)^2}{2c_\Gamma(0)}},\ \text{with}\ \ddot{c}_\Gamma(0)\triangleq\frac{d^2c_\Gamma(\tau)}{d\tau^2}\Big|_{\tau=0}.$$

We remark that since $c_\Gamma(\tau)$ is examined only for $\tau=0$, the LCR analysis may introduce non-negligible approximation errors and should be used with care. When evolving at the symbol rate, the transition probabilities between the Markov channel's states are denoted by $\Pi_{i\triangleright j}$, $i,j\le N$. In the LCR approach they are approximated as

$$\begin{cases}\Pi_{i\triangleright i+1}\approx\frac{{\rm R_c}(\zeta_{i+1})T_s}{\mathbf{p}_i} & \forall\,1\le i\le N-1,\\ \Pi_{i\triangleright i-1}\approx\frac{{\rm R_c}(\zeta_i)T_s}{\mathbf{p}_i}, & \forall\,2\le i\le N,\end{cases} \tag{26}$$

where N is the number of channel's states. Such an approximation is valid under assumptions that the LCR at the chosen thresholds is much smaller than (P_i/T_s) and that the values of SINR during symbol duration time T_s either stay in the same region i or transit to their immediate neighboring regions $i\pm1$. When satisfied, the stated assumptions allow to derive the remaining nonzero transition probabilities as

$$\begin{cases}\Pi_{1\triangleright 1}=1-\Pi_{1\triangleright 2}\\ \Pi_{N\triangleright N}=1-\Pi_{N\triangleright N-1},\\ \Pi_{i\triangleright i}=1-\Pi_{i\triangleright i-1}-\Pi_{i\triangleright i+1}\quad\text{for}\quad 2\le i\le N-1.\end{cases} \tag{27}$$

When the aforementioned assumptions are not satisfied, the channel state transition probabilities should be derived from integrating the joint PDF of the SINR over two consecutive symbol time intervals and over the desired regions [17] as

$$\Pi_{i\triangleright j}=\frac{\int_{\zeta_i}^{\zeta_{i+1}}\int_{\zeta_j}^{\zeta_{j+1}} f_\Gamma(z_{t-1},z_t)\,dz_{t-1}dz_t}{\mathbf{p}_i}, \tag{28}$$

where, from the definition of the autocovariance, the two-dimensional PDF of the Gaussian process $\Gamma(t)$ is

$$f_\Gamma(z_{t-1},z_t)=\frac{1}{2\pi\sqrt{\sigma^4_\Gamma-c^2_\Gamma(1)}}\cdot \cdot e^{-\frac{1}{2}\frac{\sigma^2_\Gamma(z_{t-1}-\eta_\Gamma)^2+\sigma^2_\Gamma(z_t-\eta_\Gamma)^2-2c_\Gamma(1)(z_{t-1}-\eta_\Gamma)(z_t-\eta_\Gamma)}{\sigma^4_\Gamma-c^2_\Gamma(1)}}.$$

Thus, thanks to the closed-form expression of $f_\Gamma(z_{t-1},z_t)$, any transition probability $\Pi_{i\triangleright j}$ can be computed numerically. The associated TPM is denoted by $\mathbf{\Pi}$. It is computed by taking into account the symbol rate, and it is defined as a stochastic $N\times N$ matrix with entries $\Pi_{i\triangleright j}$.

Since the values of $\Pi_{i\triangleright j}$ depend heavily on the choice of the thresholds delimiting the regions of SINR associated to each state of the Markov chain, in the literature on finite-state Markov channel abstractions there are different methods of partitioning the range of SINR, see e.g. [17], [35]. In this paper we consider two well known approaches for doing such methods of partitioning. The first one consists in choosing $\upsilon^{\star}_\Gamma(\varepsilon_{\rm p})$, that can be computed via (21), as the only threshold, obtaining a Markov channel with two modes, namely "good" and "bad". When the channel is in "good" mode of operation, the transmissions occur without any errors, i.e. $\eta^{\rm (g)}_{\rm M}\approx 0$ (since its exact value is by construction $\le\varepsilon_{\rm B}$), while in "bad" operational mode the channel has a probability $\eta^{\rm (b)}_{\rm M}>0$ of

presenting a failure. This model is known as Gilbert channel, see e.g. [17], [10]. In the second approach of partitioning the range of SINR, the thresholds are selected in such a way that the steady state probabilities of being in any state are equal [17], [35], i.e. $\forall i,j \leq N,\ \mathbf{p}_i = \mathbf{p}_j = (1/N)$.

As in case of analytic model of the WirelessHART link, also its finite-state abstraction should evolve at the timescale of the control-related data transmissions, and not at the timescale of individual symbols. Fortunately, the transition probabilities of channel's states in between two control-related data transmissions can be computed simply as ℓ_{E}-th power of $\mathbf{\Pi}$, since the considered Markov channel is time-homogeneous and has a finite number of states. We define this new TPM as

$$[p_{ij}]_{i,j=1}^{N} \triangleq \mathbf{P} = \mathbf{\Pi}^{\ell_{\mathrm{E}}}. \tag{29}$$

The values of p_{ij} may also be computed directly by integrating the joint PDF of the SNIR over two consecutive packet transmissions and over the desired regions, so we could write

$$p_{ij} = \frac{\int_{\zeta_i}^{\zeta_{i+1}} \int_{\zeta_j}^{\zeta_{j+1}} f_{\Gamma}\Big(z_{t-\ell_{\mathrm{E}}-1}, z_t\Big)\, dz_{t-\ell_{\mathrm{E}}-1} dz_t}{\mathbf{p}_i}. \tag{30}$$

In summary, the N-state Markov channel abstraction of the wireless link is characterized by the parameters illustrated in Table II, knowing that the first and last thresholds are by construction $\zeta_1 = -\infty$ and $\zeta_{N+1} = +\infty$.

TABLE II
CHARACTERIZATION OF AN N-STATE MARKOV CHANNEL ABSTRACTION.

Parameter	Notation
The steady state probability	$\mathbf{p}_i$
The associated PEP	$\eta_{\mathrm{M}}^{(i)}$
The thresholds	ζ_i
TPM	$\mathbf{P}$

These parameters are used to define the related **Markovian link quality metrics**: the long-run mean PEP of the Markov channel, η_{M}, is by construction equal to η_{A} since

$$\eta_{\mathrm{M}} = \sum\nolimits_{i=1}^{N} \eta_{\mathrm{M}}^{(i)} \mathbf{p}_i = \sum\nolimits_{i=1}^{N} \int_{\zeta_i}^{\zeta_{i+1}} \mathrm{R_p}(10^{\frac{\zeta}{10}}) f_{\Gamma}(\zeta)\, d\zeta, \tag{31}$$

while its long-run variance, σ_{M}^2, is given by

$$\sigma_{\mathrm{M}}^2 = \sum\nolimits_{i=1}^{N} \big(\eta_{\mathrm{M}}^{(i)}\big)^2 \mathbf{p}_i - \eta_{\mathrm{M}}^2. \tag{32}$$

To find the maximal number of consecutive packet *dropouts* with a non-negligible probability of occurrence, denoted by $\ell_{\mathrm{D}}^{\star}$, we rely on the notion of a sojourn time in a given subset of states of a discrete-time Markov process (see [36]). It is defined on a proper subset of all N states of the Markov channel, indicated by $\mathbb{S}_0$, where the packets have a non-negligible error probability, i.e. $\mathbb{S}_0 \triangleq \{\mathbf{s}_i : \eta_{\mathrm{M}}^{(i)} \geq \varepsilon_{\mathrm{P}}\}$. We denote by $\mathbb{S}_1$ the complementary subset of $\mathbb{S}_0$. $\mathbb{S}_1$ should contain at least one element. If all the states of the Markov channel have non-negligible PEP, then the analysis of the sojourn time is possible only after splitting the N-th state into two, where the new last state, denoted by $\mathbf{s}_{N+1}$, has $\eta_{\mathrm{M}}^{(N+1)} < \varepsilon_{\mathrm{B}}$. Since $\ell_{\mathrm{D}}^{\star}$ is related to the worst-case analysis, the initial state of the channel is considered to be a state in $\mathbb{S}_0$ with the largest value of the PEP. Therefore, by construction the initial probability distribution vector v_0 has 1 in correspondence of $\mathbf{s}_1$, and 0 everywhere else. The partition $\{\mathbb{S}_0, \mathbb{S}_1\}$ of the state space of the Markov channel induces a decomposition of its TPM $\mathbf{P}$ into four submatrices:

$$\mathbf{P} = \begin{bmatrix} \mathbf{P}_{00} & \mathbf{P}_{01} \\ \mathbf{P}_{10} & \mathbf{P}_{11} \end{bmatrix}, \quad \text{with} \quad \mathbf{P}_{\mathrm{AB}} \triangleq [p_{ij}]_{i,j:i\in\mathbb{S}_{\mathrm{A}}, j\in\mathbb{S}_{\mathrm{B}}}, \tag{33}$$

where $\mathrm{A}, \mathrm{B} \in \{0,1\}$. Accordingly, the probability of having ℓ_{D} consecutive dropouts during k-th visit of partition $\mathbf{P}_{00}$ is

$$\Delta(\ell_{\mathrm{D}}, k) = \mathrm{v}_0 \left((\mathbb{I} - \mathbf{P}_{00})^{-1} \mathbf{P}_{01} (\mathbb{I} - \mathbf{P}_{11})^{-1} \mathbf{P}_{10}\right)^{k-1} \cdot \cdot \mathbf{P}_{00}^{\ell_{\mathrm{D}}-1} (\mathbb{I} - \mathbf{P}_{00})\, \mathbf{1}, \tag{34}$$

where $\mathbb{I}$ is the identity matrix of the appropriate size. Then, $\ell_{\mathrm{D}}^{\star}$ is obtained as the solution of the optimization problem

$$\max(\ell_{\mathrm{D}}), \quad \text{subject to} \quad \Delta(\ell_{\mathrm{D}}, k) \geq \varepsilon_{\mathrm{B}},\ k \geq 0. \tag{35}$$

In summary, the Markovian LQMs listed in Table III can be compared with the LQMs characterizing the analytic model of the radio link (see Table I), permitting us to evaluate and validate this finite-state model of the WirelessHART in straightforward manner. In the next sections we will show on a case study from the automatic control domain how the quality metrics permit to find a high fidelity finite-state abstraction of the analytic channel useful for solving networked control problems.

TABLE III
MARKOVIAN LQMS.

Link quality metric	Notation
The long-run mean PEP	η_{M}
The long-run variance of PER	σ_{M}^2
The maximal number of consecutive dropouts	$\ell_{\mathrm{D}}^{\star}$

III. OPTIMAL CONTROL OVER A WIRELESSHART LINK

To show the importance of the accurate Markov channel model for the WNCSs, we examine the inverted pendulum (on a cart) described in [37], which is controlled remotely over a WirelessHART link presented in the previous section. We model it as a linear stochastic system with intermittent control packets due to the lossy communication channel [14]:

$$x_{k+1} = Ax_k + Bu_k^a + w_k \quad \text{with} \quad u_k^a = \nu_k u_k^c, \tag{36}$$

where, x_k is a system state, u_k^a is the control input to the actuator, A and B are state and input matrices of appropriate size, respectively, u_k^c is the desired control input computed by the controller, w_k is Gaussian white process noise (with zero mean and covariance matrix Σ_w) assumed to be independent from the initial state x_0 and from the stochastic variable ν_k, which models the packet loss between the controller and the actuator: if the packet is correctly delivered then $u_k^a = u_k^c$, otherwise if it is lost then the actuator does nothing, i.e., $u_k^a = 0$. We assume full state observation with no measurement noise, and no observation packet loss, so the optimal control must necessarily be a static state feedback and no filter is necessary.

In such a setting we compare the performance of two state feedback controllers, both designed to minimize the cost function, which can be described by

$$J_* = \lim_{t\to\infty} \sup \frac{1}{t} \mathbb{E}\Big[\sum\nolimits_{k=0}^{t} (x_k^* Q x_k + u_k^{a*} R u_k^a)\Big], \tag{37}$$

where $Q \succeq 0$ and $R \succ 0$ are the state and control weighting matrices, respectively.

The first state-feedback controller is derived in [14], treating ν_k as i.i.d. Bernoulli random variables. The obtained state-independent controller and the value of the related performance index will be denoted respectively as $K^b_\star, J^b_\star$.

The second controller is the optimal linear quadratic regulator for a MJLS in the presence of one time-step delayed mode observations [18]. It considers ν_k as a random variable governed by the Markov channel, where the probability of the successful packet delivery is conditioned to the state of the communication link, i.e., $\Pr(\nu_k = 1 \mid \theta_k = \mathbf{s}_i) = \hat{\nu}_i$, while the probability of the packet loss is $\Pr(\nu_k = 0 \mid \theta_k = \mathbf{s}_i) = 1 - \hat{\nu}_i$. The operational modes are observed by controller via ACKs that are available only after the current decision on the controller gain to apply has been made and sent through the channel, since the actual success of the transmission is not known in advance. We assume that ACKs, and also the communication channel states (measured through SINR), are not received at the controller instantaneously, but become available before the next decision on the control to apply. This means that the state-space representation of the MJLS in closed-loop becomes

$$x_{k+1} = \left(A + \nu_{\theta_k} B K^c_{\theta_{k-1}}\right) x_k + w_k \tag{38}$$

where $K^c_{\theta_{k-1}}$ is a mode-dependent state-feedback controller, computed as in [18]. The value of the related performance index will be denoted as $J^c_\star$.

To be of any practical use, the system should remain always stable in closed-loop. To check whether the controlled system is actually stable, we adopt the techniques from the theory of discrete-time MJLSs [38]. In particular, we rely on [19], which shows that a MJLS with one time-step delayed mode observations is mean square stable if and only if the spectral radius ρ of the characteristic matrix $\mathbf{\Lambda}$ is smaller than 1, being

$$\mathbf{\Lambda} = \left(\bigoplus_{j=1}^{N}\left(\bigoplus_{i=1}^{N} p_{ij}\right)\right)' \otimes \left(\bigoplus_{j=1}^{N}(A \otimes A)\right) + \left(\bigoplus_{j=1}^{N}\left(\bigoplus_{i=1}^{N} \hat{\nu}_i p_{ij}\right)\right)' \otimes \left(\bigoplus_{j=1}^{N}\Big(\big((BK_j)\otimes(BK_j)\big) + \big((BK_j)\otimes A\big) + \big(A\otimes(BK_j)\big)\Big)\right),$$

where, as before, p_{ij} is the probability of transition between the Markov channel's states, $\otimes$ indicates the Kronecker product, $\oplus$ the direct sum, and $\oplus$ the horizontal concatenation of two matrices with the same number of rows.

In Section IV-C we will check the stability of the closed-loop system through the computation of $\rho(\mathbf{\Lambda})$, and verify it via a statistical analysis.

IV. Numerical case study

The parameters of our inverted pendulum shown in Fig. 3 are summarized in Table IV. The state variables are the cart position coordinate x and pendulum's angle from vertical ϕ, together with respective first derivatives. We are interested in designing a controller that stabilizes the pendulum in up-right position, corresponding to unstable equilibrium point $\mathrm{x}^\star = 0\,\mathrm{m}$, $\phi^\star = 0$ rad, so the system state is defined by $x = \left[\delta\mathrm{x}, \delta\dot{\mathrm{x}}, \delta\phi, \delta\dot{\phi}\right]'$,

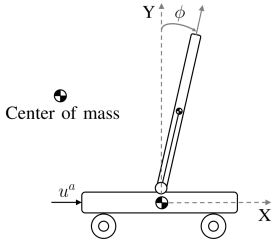

Fig. 3. The inverted pendulum on a cart.

TABLE IV
The parameters of the inverted pendulum on a cart.

Parameter	Notation
The cart mass	$0.5\,\mathrm{kg}$
The pendulum mass	$0.2\,\mathrm{kg}$
The inertia about the pendulum mass center	$0.006\,\mathrm{kg}$
The distance from the pivot to the mass center	$0.3\,\mathrm{m}$
The friction coefficient of the cart	$0.1\,\mathrm{N{\cdot}s/m}$

where $\delta\mathrm{x}(t) = \mathrm{x}(t) - \mathrm{x}^\star$, $\delta\phi(t) = \phi(t) - \phi^\star$. This determines the frame length of the control-related messages: $\ell_{\mathrm{F}} = 208$ bits. It is assumed that the initial state x_0 equals $\left[0, 0, \frac{\pi}{10}, 0\right]'$. The process noise is characterized by the covariance matrix $\Sigma_w = vv'$, with $v = [0.030, 0.100, 0.010, 0.150]'$. To prioritize the goal of maintaining the inverted pendulum in the upright position, we use the following weighting matrices for all the control schemes being compared: $Q = \oplus(1, 0.1, 100, 0.1)$ and $R = 1$, so that the weight associated to $\delta\phi(t)$ is much larger than all other weights. The inverted pendulum on a cart moves in a direction orthogonal to both its remote controller and the transmitter that creates interference. We set the noise figure F_n of the receiver to $23.8\,\mathrm{dB}$ (so that its sensitivity is just above $-85\,\mathrm{dBm}$ as required by the standard [21]). Thus, the noise spectral density $N_0 = k_B T_0 F_n$, where k_B is the Boltzmann's constant and T_0 is standard noise temperature. The values of other channel parameters used in this case study are summarized in Table V, where ε_1 denotes the machine epsilon, and ε_{p} is the probability of one data packet loss in a century of continuous operation with the sampling time of T_u (measured in seconds).

A. Case 1

The first case describes the scenario, where the minimum update period of the WirelessHART standard is considered for the control application, i.e., $T_u = 0.1\,\mathrm{s}$. The distance between the transmitter-receiver pair of interest, d_0, and the distance between the interfering Tx and the reference user, d_1, have the values shown in Table V. According to these values, we have $\ell_{\mathrm{E}} = 60$, and the implicit analytic model of the channel is characterized by the Gaussian process described in Table VI. We underline that $c_{\Gamma_1}(61) = 0$. This means that at the packet level two consecutive data transmissions are independent, so the i.i.d. Bernoulli distribution is appropriate to model packet losses. The analytic LQMs are also outlined in Table VI.

To show the usefulness of the derived link quality metrics, we first construct a three-state Markov model with equiprob-

TABLE V
PARAMETER VALUES FOR CASE STUDY.

Parameter	Notation	Value			Unit	Reference
		Case 1	*Case 2*	*Case 3*		
Symbol rate	$1/T_s$	62.5			ksymb/s	[27]
Chip rate	$1/T_c$	2			Mchip/s	[27]
Channel bandwidth	W	2			MHz	[24]
Users speed	v_0, v_1	5.37			m/s	Pendulum
Shadowing decay dist.	d_{c_0}, d_{c_1}	9			m	[23]
Shadowing std. dev.	$\sigma_{\beta_0}, \sigma_{\beta_1}$	2			dB	[39]
PCE std. dev.	$\sigma_{e_0}, \sigma_{e_1}$	1.5			dB	[31]
PCE decorr. time	$\tau_{\xi_0}, \tau_{\xi_1}$	$1.52 \cdot 10^{-3}$			s	[31]
Ref. user Tx power	P_0	0			dBm	[21]
Interf. Tx power	P_1	10			dBm	[21]
Dist. ref. Tx-Rx pair	d_0	6	6	10	m	Indoor: 1–10 m [23]
Dist. interf. Tx-Rx pair	d_1	10	10	4	m	
Publish data message update period	T_u	100	5	5	ms	[21]
Negligible PER threshold	ε_{P}	$\frac{1}{(1/T_u)\cdot 3600\cdot 24\cdot 36525}$			scalar	Design choice
Negligible packet error burst threshold	ε_{B}	$100\varepsilon_1$			scalar	

TABLE VI
RESULTS OF CASE STUDY.

	Parameter	Case 1	Case 2	Case 3
Gaussian process	μ	6.331	6.331	-9.061
	σ^2	42.504	42.504	42.505
	ℓ_{E}	60	3	3
	$c_\Gamma(1)$	19.825	19.825	19.826
	$c_\Gamma(\ell_{\mathrm{E}}+1)$	0	1.373	1.373
Analytic LQMs	η_{A}	0.113	0.113	0.871
	σ^2_{A}	0.087	0.087	0.098
	$\ell^\star_{\mathrm{B}}(\varepsilon_{\mathrm{B}}, \varepsilon_{\mathrm{P}})$	36	40	2270
Gilbert channel abstraction	$\mathbf{p}_i$	$(0.413, 0.587)$	$(0.437, 0.563)$	$(0.986, 0.014)$
	$\eta^{(i)}_{\mathrm{M}}$	$(0.274, 0)$	$(0.258, 0)$	$(0.883, 0)$
	$\zeta_2 = \upsilon^\star_\Gamma(\varepsilon_{\mathrm{P}})$	4.889	5.302	5.302
	$\mathbf{P}$	$\begin{bmatrix} 0.413 & 0.587 \\ 0.413 & 0.587 \end{bmatrix}$	$\begin{bmatrix} 0.454 & 0.546 \\ 0.4246 & 0.575 \end{bmatrix}$	$\begin{bmatrix} 0.986 & 0.014 \\ 0.9846 & 0.015 \end{bmatrix}$
Markovian LQMs	η_{M}	0.113	0.113	0.871
	σ^2_{M}	0.018	0.016	0.011
	$\ell^\star_{\mathrm{D}}$	36	40	2011

able partitioning of the range of SINR, as introduced in Section II-E. Specifically, the range of SINR is partitioned in such a way that the steady state probabilities of being in any state are equal. The related TPM is derived from either LCR analysis via (26) and (27), or by integrating $f_{\Gamma_1}(z_{t-1}, z_t)$. We have for both approaches that

$$\begin{cases} (\mathbf{p}_i)_{i=1}^3 = (1/3, 1/3, 1/3)\,, \\ (\zeta_i)_{i=1}^4 = (-\infty, 3.522, 9.139, \infty)\,, \\ (\eta^{(i)}_{\mathrm{M}})_{i=1}^3 = (0.339, 4.4 \cdot 10^{-9}, 0)\,. \end{cases} \tag{39}$$

Therefore, from (31) and (32) we get respectively $\eta_{\mathrm{M}} = 0.113$ and $\sigma^2_{\mathrm{M}} = 0.026$. TPMs describing the evolution of the Markov channel at the symbol rate, denoted by $\mathbf{\Pi}_i$, and TPMs of the Markov channel evolving at the packet rate, $\mathbf{P}_i$, (with $i = \mathrm{L}$ when the transition probabilities are obtained from the LCR analysis, and $i = \mathrm{I}$ when the integration of $f_{\Gamma_1}(z_{t-1}, z_t)$ is used) are

$$\mathbf{\Pi}_{\mathrm{L}} = \begin{bmatrix} 0.997 & 0.003 & 0 \\ 0.003 & 0.994 & 0.003 \\ 0 & 0.003 & 0.997 \end{bmatrix}, \mathbf{\Pi}_{\mathrm{I}} = \begin{bmatrix} 0.532 & 0.315 & 0.153 \\ 0.3146 & 0.371 & 0.3146 \\ 0.153 & 0.315 & 0.532 \end{bmatrix};$$

$$\mathbf{P}_{\mathrm{L}} = \begin{bmatrix} 0.846 & 0.141 & 0.013 \\ 0.141 & 0.717 & 0.141 \\ 0.013 & 0.141 & 0.846 \end{bmatrix}, \mathbf{P}_{\mathrm{I}} = \begin{bmatrix} 1/3 & 1/3 & 1/3 \\ 1/3 & 1/3 & 1/3 \\ 1/3 & 1/3 & 1/3 \end{bmatrix}.$$

Importantly, the values of $\mathbf{P}_{\mathrm{I}}$ show that at the packet level two consecutive data transmissions are independent, while the structure of $\mathbf{P}_{\mathrm{L}}$ erroneously indicates the correlation between the channel states. Fortunately, the difference in the maximal number of consecutive dropouts helps to discover this mistake, since (for the same values of ε_{B}, ε_{P}) we have that $\ell^\star_{\mathrm{D_L}} = 441$, $\ell^\star_{\mathrm{D_I}} = 77$, while from the application of either (22), or (23), we have that $\ell^\star_{\mathrm{B_1}} = 36$. This discrepancy in the values of $\ell^\star_{\mathrm{D}}$ and $\ell^\star_{\mathrm{B}}$ also indicates that the simple equiprobable partitioning of the range of SINR is not the best choice, since it does not consider the value of $\upsilon^\star_{\Gamma_1}(\varepsilon_{\mathrm{P}})$ in deriving the thresholds ζ_i.

Consequently, we consider also a Gilbert model of the WirelessHART link. Henceforth we will use only the integration of the joint PDF of the SINR over two consecutive packet transmissions to compute exact values of TPMs $\mathbf{P}$ directly, via (30). The characteristics of the obtained Gilbert channel abstraction of the radio link and its LQMs are reported in Table VI. Notably, we have that $\ell^\star_{\mathrm{D_1}} = 36$, and also $\ell^\star_{\mathrm{B_1}} = \ell^\star_{\mathrm{B}}(\varepsilon_{\mathrm{B_1}}, \varepsilon_{\mathrm{P}}) = 36$. Therefore, as expected, the Gilbert channel is well suited for studying the maximal number of consecutive dropouts.

B. Case 2

The minimum update period $T_u = 0.1$ s of the WirelessHART standard is too slow for several control applications and it makes the wireless link uncorrelated at the packet level. Thus, in view of the continuous development of mobile network technologies that support much higher update rates, we consider $T_u = 0.005$ s, i.e. Case 2 in Table V. The characteristics of the implicit analytic model of the radio link and of its finite-state abstraction via Gilbert model are reported in Table VI. We notice that the higher update rate does not change the values of η_Γ, σ^2_Γ, and $c_\Gamma(\tau)$, which are computed via (16). Accordingly, also the values of η_{A} and σ^2_{A}, that are obtained respectively through (19) and (20), remain the same as before. However, with ℓ_{E} being equal to 3, we have $c_{\Gamma_1}(4) = 1.373$: there is a correlation between the control-related transmissions. Since a smaller value of ε_{P} is used in this case, then $\upsilon^\star_{\Gamma_2}(\varepsilon_{\mathrm{P}}) = 5.302$. Therefore, the lower bound of $\ell^\star_{\mathrm{B_2}}$ computed via (23) becomes 39 while its exact value obtained from (22) is 40. The associated Gilbert channel, with characteristics and LQMs shown in Table VI, is still able to closely track the behavior of the analytic model, which is evident from the comparison of the respective LQMs.

C. Case 3

Finally, this last case shows the real utility of the accurate finite-state Markov channel models in networked control applications. This scenario describes the situation with a sustained

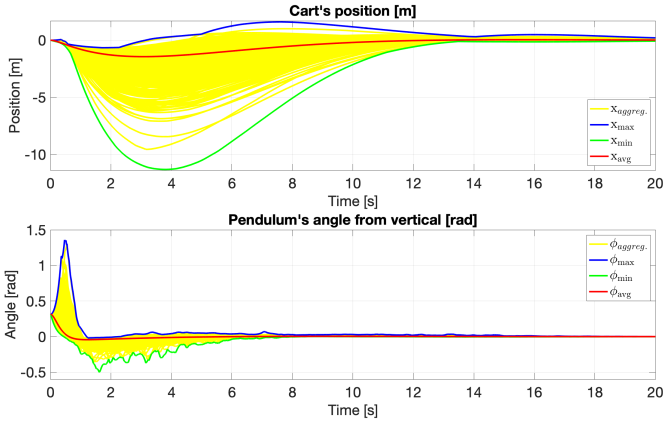

Fig. 4. Traces of the systems state that are generated under the Markovian control law over the analytic WirelessHART channel.

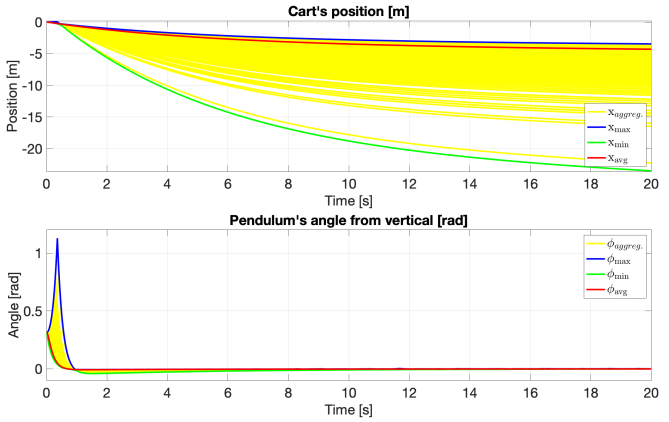

Fig. 5. Traces of the systems state that are generated under the Bernoulli control law over the same analytic WirelessHART channel.

jamming activity. The analytic and Gilbert channel abstraction have the values depicted in Table VI, where $\ell^{\star}_{\mathrm{B}_3} = 2270$ is computed via (22), while its lower bound from (23) is 2263. The discrepancy with $\ell^{\star}_{\mathrm{D}_3} = 2011$ is due to the numerical precision of the operations involved in computing (34).

We consider the networked control application implemented over this link, and analyze the performance of both the optimal linear quadratic regulation with Bernoulli and Gilbert abstractions of the analytic wireless channel. The state space representation (38) of the controlled system linearized about the unstable equilibrium point and discretized with sampling period $T_u = 0.005\,\mathrm{s}$ is defined by

$$A = \begin{bmatrix} 1 & 0.005 & 0 & 0 \\ 0 & 0.999 & 0.013 & 0 \\ 0 & 0 & 1 & 0.005 \\ 0 & -0.002 & 0.156 & 1 \end{bmatrix}, \; B = \begin{bmatrix} 0 \\ 0.009 \\ 0 \\ 0.023 \end{bmatrix}.$$

The matrix A is unstable, since its eigenvalues are $\mathrm{eig}(A) = (1.028, 1.000, 0.999, 0.972)$. It is easy to verify that $R \succ 0$, $Q \succeq 0$, and the pairs (A, B) and (A, Q) are controllable, so the closed-loop system is asymptotically stable, when $\nu_k = 1$ for all k. The critical probability ν_c for the networked control over Bernulli channel [14] for this system is $0.\mathbf{053}$, so that maximal length of the fading sequence with the probability of occurrence larger than ε_{B} is 573, i.e. it is much smaller then 2270. Still, since $\hat{\nu} = 1 - \eta_{\mathrm{A}_3} > \nu_c$, we may try to apply the controller K^b as in [14]. We obtain $K^b = [0.024, -3.252, 255.665, 45.958]$, $J^b_{\star} = 1.25 \cdot 10^6$. By checking the stability of this controller when applied to a Gilbert channel case, we find out that $\rho(\mathbf{\Lambda}^b) = 1.000065 > 1$, so the system is unstable. If we exploit the information available from the Gilbert channel to construct a MJLS with one time-step delayed mode observations presented at the beginning of this section, we obtain $K^c_1 = [-0.754, -3.668, 114.502, 20.698]$, $K^c_2 = [-0.764, -3.713, 115.912, 20.953]$, so that $J^c_{\star} = 451.124$. This controller stabilizes the system, since $\rho(\mathbf{\Lambda}^c) = 0.997 < 1$.

To validate the presented results, we have simulated the behavior of the inverted pendulum on a cart, with a remote controller implementing either the Bernoulli, or Markovian control law, and sending the data over the analytic WirelessHART channel. Specifically, we randomly generated 10000 admissible evolutions (each one with 4000 samples accounting for 20s of operation) of the analytic channel, and used them for both control strategies. Since both Bernoulli and Markovian controllers do not consider any constraints on the system states or control inputs, all the physics-related constraints were neglected in our simulations. Figs. 4 and 5 depict statistical results of our simulations: it is evident that Fig. 4 shows a stable system behavior of the inverted pendulum on a cart when it is governed by the remote Markovian controller, while the behavior of the pendulum controlled remotely by a Bernoulli strategy, that is reported in Fig. 5, is clearly unstable, as it was expected from our analysis of stability conditions based on the spectral radius of the characteristic matrices.

V. Conclusions

In this paper, we have presented a mathematical framework for deriving an accurate Markov channel model of a WirelessHART radio link affected by path loss, shadowing, power residual control and persistent interference. We also introduced link quality metrics that permit us to asses how good a finite-state representation of the radio link is. We have shown on a numerical case study how these metrics are essential for an easy discovering of some pitfalls related to both the choice of the method of partitioning of the range of signal-to-interference-plus-noise ratio and the computation of transition probabilities between operational modes of the Markov channel. We have also demonstrated in a formal setting that an accurate Markov model of the WirelessHART link allows us to design a controller that guarantees stability and improves control performance of the closed-loop system, where other approaches based on a simplified channel model fail. Further work is being done to account for a more general communication scenario and to compare different SINR partitioning methods for improving the wireless channel model.

References

[1] P. Park, S. C. Ergen, C. Fischione, C. Lu, and K. H. Johansson, "Wireless network design for control systems: A survey," *IEEE Commun. Surveys Tut.*, vol. 20, no. 2, pp. 978–1013, 2018.

[2] O. Bello and S. Zeadally, "Intelligent device-to-device communication in the Internet of things," *IEEE Syst. J.*, vol. 10, no. 3, pp. 1172–1182, 2016.

[3] J. Sztipanovits, X. Koutsoukos, G. Karsai, N. Kottenstette, P. Antsaklis *et al.*, "Toward a science of cyber–physical system integration," *Proc. IEEE*, vol. 100, no. 1, pp. 29–44, 2012.

[4] M. Wollschlaeger, T. Sauter, and J. Jasperneite, "The future of industrial communication: Automation networks in the era of the Internet of Things and Industry 4.0," *IEEE Ind. Electron. Mag.*, vol. 11, no. 1, pp. 17–27, 2017.

[5] F. Smarra, A. D'Innocenzo, and M. D. Di Benedetto, "Fault tolerant stabilizability of MIMO multi-hop control networks," *IFAC Proc.*, vol. 45, no. 26, pp. 79–84, 2012, 3rd IFAC Workshop Distrib. Estimation Control Netw. Syst.

[6] A. Willig, K. Matheus, and A. Wolisz, "Wireless technology in industrial networks," *Proc. IEEE*, vol. 93, no. 6, pp. 1130–1151, 2005.

[7] A. Ahlén, J. Akerberg, M. Eriksson, A. J. Isaksson, T. Iwaki *et al.*, "Toward wireless control in industrial process automation: A case study at a paper mill," *IEEE Control Syst. Mag.*, vol. 39, no. 5, pp. 36–57, 2019.

[8] A. Sikora and V. F. Groza, "Coexistence of IEEE 802.15.4 with other systems in the 2.4 GHz-ISM-Band," in *IEEE Instrum. Meas. Technol. Conf.*, vol. 3, May 2005, pp. 1786–1791.

[9] S. Zacharias, T. Newe, S. O'Keeffe, and E. Lewis, "A lightweight classification algorithm for external sources of interference in IEEE 802.15.4-based wireless sensor networks operating at the 2.4 GHz," *Int. J. Distrib. Sensor Netw.*, vol. 10, no. 9, pp. 1–24, 2014.

[10] A. P. Gonçalves, A. R. Fioravanti, and J. C. Geromel, "Markov jump linear systems and filtering through network transmitted measurements," *Signal Process.*, vol. 90, no. 10, pp. 2842–2850, 2010.

[11] C. Lu, A. Saifullah, B. Li, M. Sha, H. Gonzalez *et al.*, "Real-time wireless sensor-actuator networks for industrial cyber-physical systems," *Proc. IEEE*, vol. 104, no. 5, pp. 1013–1024, May 2016.

[12] J. P. Hespanha, P. Naghshtabrizi, and Y. Xu, "A survey of recent results in networked control systems," *Proc. IEEE*, vol. 95, no. 1, pp. 138–162, 2007.

[13] W. M. H. Heemels, A. R. Teel, N. van de Wouw, and D. Nesic, "Networked control systems with communication constraints: Tradeoffs between transmission intervals, delays and performance," *IEEE Trans. Autom. Control*, vol. 55, no. 8, pp. 1781–1796, 2010.

[14] L. Schenato, B. Sinopoli, M. Franceschetti, K. Poolla, and S. S. Sastry, "Foundations of control and estimation over lossy networks," *Proc. IEEE*, vol. 95, no. 1, pp. 163–187, 2007.

[15] V. Gupta, A. F. Dana, J. P. Hespanha, R. M. Murray, and B. Hassibi, "Data transmission over networks for estimation and control," *IEEE Trans. Autom. Control*, vol. 54, no. 8, pp. 1807–1819, 2009.

[16] M. Pajic, S. Sundaram, G. J. Pappas, and R. Mangharam, "The wireless control network: a new approach for control over networks," *IEEE Trans. Autom. Control*, vol. 56, no. 10, pp. 2305–2318, 2011.

[17] P. Sadeghi, R. Kennedy, P. Rapajic, and R. Shams, "Finite-state Markov modeling of fading channels – a survey of principles and applications," *IEEE Signal Process. Mag.*, vol. 25, no. 5, pp. 57–80, 2008.

[18] I. Matei, N. C. Martins, and J. S. Baras, "Optimal linear quadratic regulator for Markovian jump linear systems, in the presence of one time-step delayed mode observations," *IFAC Proc.*, vol. 41, no. 2, pp. 8056–8061, 2008, 17th IFAC World Congr.

[19] Y. Zacchia Lun and A. D'Innocenzo, "Stabilizability of Markov jump linear systems modeling wireless networked control scenarios," in *IEEE Conf. Decision Control (CDC), Preprints*, 2019, pp. 5766–5772, also available on arXiv at https://arxiv.org/abs/1907.12403.

[20] D. Chen, M. Nixon, and A. Mok, *WirelessHART™*. Springer, 2010.

[21] BSI Standards Publication BS EN 62591:2016, *Industrial communication networks – Wireless communication network and communication profiles – WirelessHART™*, it is identical to IEC 62591:2016.

[22] A. Alrish, Y. Zacchia Lun, A. D'Innocenzo, and F. Santucci, "Work in progress: Systematic derivation of accurate analytic markov channel models for industrial control," in *IEEE Int. Workshop Factory Commun. Syst. (WFCS)*, May 2019, pp. 1–4.

[23] A. Goldsmith, *Wireless Communications*. CUP, 2005.

[24] IEEE Std 802.15.4™-2006, *Standard for Information technology – Local and metropolitan area networks – Specific requirements – Part 15.4: Wireless MAC and PHY Specifications for Low-Rate WPANs*.

[25] N. Jaldén, P. Zetterberg, B. Ottersten, A. Hong, and R. Thoma, "Correlation properties of large scale fading based on indoor measurements," in *IEEE Wireless Commun. Netw. Conf. (WCNC)*, 2007, pp. 1894–1899.

[26] A. Seetharam, J. Kurose, D. Goeckel, and G. Bhanage, "A Markov chain model for coarse timescale channel variation in an 802.16e wireless network," in *IEEE Conf. Comput. Commun. (INFOCOM)*, 2012, pp. 1800–1807.

[27] HART Communication Foundation document number HCF_SPEC-065, *2.4 GHz DSSS O-QPSK Physical Layer Specification*, Sept. 2007.

[28] F. Santucci, G. Durastante, F. Graziosi, and C. Fischione, "Power allocation and control in multimedia CDMA wireless systems," *Telecommun. Syst.*, vol. 23, no. 1–2, pp. 69–94, 2003.

[29] F. Santucci and F. Graziosi, "Power allocation in a multimedia CDMA wireless system with imperfect power control," in *IEEE Int. Conf. Commun. (ICC)*, vol. 3, 1999, pp. 1668–1672.

[30] F. Graziosi, L. Fuciarelli, and F. Santucci, "Second order statistics of the SIR for cellular mobile networks in the presence of correlated co-channel interferers," in *IEEE Veh. Technol. Conf. (VTC)*, vol. 4, 2001, pp. 2499–2503.

[31] C. Fischione, F. Graziosi, and F. Santucci, "Approximation for a sum of On-Off log-normal processes with wireless applications," *IEEE Trans. Commun.*, vol. 55, no. 9, pp. 1822–1822, Sept. 2007.

[32] A. Genz and F. Bretz, *Computation of multivariate normal and t probabilities*, ser. Lecture Notes Statist. Springer, 2009, vol. 195.

[33] Z. I. Botev, "The normal law under linear restrictions: simulation and estimation via minimax tilting," *J. Roy. Statistical Soc.: Series B (Statistical Methodology)*, vol. 79, no. 1, pp. 125–148, 2017.

[34] G. L. Stüber, *Principles of mobile communication*. Springer, 2017.

[35] J. G. Ruiz, B. Soret, M. C. Aguayo-Torres, and J. T. Entrambasaguas, "On finite state Markov chains for Rayleigh channel modeling," in *Wireless Commun., Veh. Technol., Inf. Theory Aerosp. Electron. Syst. Technol. (Wireless VITAE)*, 2009, pp. 191–195.

[36] G. Rubino and B. Sericola, "Sojourn times in finite Markov processes," *J. Appl. Probability*, vol. 26, no. 4, pp. 744–756, 1989.

[37] G. F. Franklin, J. D. Powell, and A. Emami-Naeini, *Feedback control of dynamic systems*, 6th ed. Prentice Hall, 2009.

[38] O. L. V. Costa, M. D. Fragoso, and R. P. Marques, *Discrete-time Markov jump linear systems*. Springer, 2005.

[39] S. Yao and E. Geraniotis, "Optimal power control law for multimedia multirate CDMA systems," in *IEEE Veh. Technol. Conf. (VTC)*, vol. 1. IEEE, 1996, pp. 392–396.